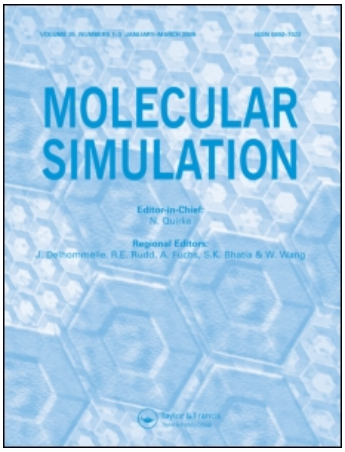

Molecular Simulation
Publication details, including instructions for authors and subscription information:
http://www.informaworld.com/smpp/title~content=t713644482

Prediction of Conformational Free Energy Differences of Solutes in Solution: An MC-MST Study

B. Hernández[a]; C. Curutchet[a]; C. Colominas[a]; M. Orozco[a]; F. J. Luque[a]
[a] Departament de Bioquímica, Facultat de Química, Universitat de Barcelona, Barcelona, Spain

Online publication date: 26 October 2010

To cite this Article Hernández, B. , Curutchet, C. , Colominas, C. , Orozco, M. and Luque, F. J.(2002) 'Prediction of Conformational Free Energy Differences of Solutes in Solution: An MC-MST Study', Molecular Simulation, 28: 1, 153 — 171
To link to this Article: DOI: 10.1080/08927020211979
URL: http://dx.doi.org/10.1080/08927020211979

Molecular Simulation, 2002, Vol. 28(1–2), pp. 153–171

PREDICTION OF CONFORMATIONAL FREE ENERGY DIFFERENCES OF SOLUTES IN SOLUTION: AN MC-MST STUDY

B. HERNÁNDEZ[a], C. CURUTCHET[b], C. COLOMINAS[c], M. OROZCO[a,*] and F. J. LUQUE[b,†]

[a]*Departament de Bioquímica, Facultat de Química, Universitat de Barcelona, Av. Martí i Franqués 1, E-08028, Barcelona, Spain;* [b]*Departament de Físico-Química, Facultat de Farmàcia, Universitat de Barcelona, Av. Diagonal s/n, E-08028, Barcelona, Spain;* [c]*Institut Químic de Sarrià, Universitat Ramon Llull, Via Augusta 390, Barcelona 08017, Spain*

(Received August 2000; accepted February 2001)

This study reports an extension of the MC-MST method to explore the conformational space of molecules in condensed phases. The MC-MST method combines a Monte Carlo (MC) Metropolis algorithm to sample the conformational space with the semiclassical version of the Miertus-Scrocco-Tomasi (MST) continuum model to treat solvation effects. The extension of the MC-MST method to describe the solvent-induced changes in the conformational space is examined for 1,2-dichloroethane and the two tautomers of neutral histamine. The results allow us to discuss the capabilities of the MC-MST method to reproduce the conformational preferences of molecules in solution.

Keywords: Solvation; Conformational sampling; Monte carlo; Continuum model

1. INTRODUCTION

Solvation plays a key role in determining the structural and reactive properties of molecules [1–3]. In particular, the conformational properties of flexible molecules can be largely influenced by the solvent (for instance,

*e-mail: mailto:modesto@luz.bq.ub.es
†Corresponding author. e-mail: mailto:javier@far1.far.ub.es

ISSN: 0892-7022 DOI: 10.1080/08927020290004430

see Ref. [4]), and in some cases complete conformational shifts occur upon transfer from the gas phase to condensed phases.

Theoretical methods are valuable to interpret solvent effects on the conformational properties of molecules [5–10]. Discrete-classical methods based on molecular dynamics (MD) and Monte Carlo (MC) algorithms give a suitable description of the condensed phase. Combined with statistical mechanical techniques, they are very powerful to predict free energy differences associated with conformational changes [6–9]. They are, nevertheless, computationally very demanding, since the simulation must be run long enough to avoid any *bias* in the sampling due to the starting configuration of the system, and to allow the system to surpass barriers connecting multiple minima. Furthermore, most of the computer time is spent in sampling the solvent configurational space, and only a fraction of the computational effort involves the exploration of the internal degrees of freedom of the solute. Despite the advent of technical improvements and the increase in the computer power that have occurred in the last years, much progress is still necessary to widen the range of systems whose conformational space can be studied by means of these methods. Another possibility for the representation of the solute conformational space in solution relies on the use of continuum models of solvation (for review, see Refs. [1] and [10]). In this approach the solute is considered at atomic detail, but the solvent is represented as a continuum. The combination of the continuum approach with MD or MC approaches can provide a useful alternative to discrete methods to represent flexible molecules in solution [11–14].

In this paper we extend the MC-MST method to the analysis of the conformational of molecules in solution. The MC-MST method is based on the combination of our semiclassical version [15] of the Miertus-Scrocco-Tomasi (MST, also named PCM; see Refs. [10] and [16]) method with a Metropolis-Monte Carlo program. The rest of the article is organized as follows. In Section 2 a review of the MC-MST method is made. Particular attention is paid to the treatment of solvation by the semiclassical MST model. Section 3 reviews previous applications of the MC-MST method to molecular recognition. Section 4 reports the extension of the MC-MST method to investigate conformational equilibria in solution. This is exemplified for the *gauche*/*trans* equilibrium of 1,2-dichloroethane, and the conformational preference of the N1—H and N3—H tautomers of neutral histamine. Finally, a brief discussion of the capabilities of the MC-MST method is made in Section 5.

2. THE MC-MST METHOD

2.1. Energy Functional

For a given molecular configuration, the MC-MST method determines an effective energy, E_{ef}, obtained by the sum of the internal energy, E_{int}, of the molecular system and its free energy of solvation, ΔG_{sol}, Eq. (1). Since the aim of the MC-MST method is to perform an exhaustive sampling of the configurational space, both E_{int} and ΔG_{sol} are computed within a classical framework. Thus, the internal energy is evaluated using a classical force-field, and the free energy of solvation is computed using the semiclassical MST model.

$$E_{ef} = E_{int} + \Delta G_{sol} \tag{1}$$

2.2. The Semiclassical MST Method

The MST continuum method determines ΔG_{sol} as the addition of three contributions Eq. (1): cavitation (ΔG_{cav}), van der Waals (ΔG_{vW}), and electrostatic (ΔG_{ele}).

$$\Delta G_{sol} = \Delta G_{cav} + \Delta G_{vW} + \Delta G_{ele} \tag{2}$$

The free energy of cavitation is computed using Pierotti's scaled particle theory [17] adapted to molecular shaped cavities according to the procedure proposed by Claverie (see Eq. (3); Ref. [18]). In Eq. (3) $\Delta G_{P,i}$ is the cavitation free energy of atom i in Pierotti's formalism, S_i is the solvent-exposed surface of atom i, S_T is the total solvent-exposed surface of the molecule, N is the number of atoms, and $\Delta G_{C-P,i}$ is the Claverie-Pierotti contribution of atom i.

$$\Delta G_{cav} = \sum_{i=1}^{N} \Delta G_{C\text{-}P,i} = \sum_{i=1}^{N} \frac{S_i}{S_T} \Delta G_{P,i} \tag{3}$$

The van der Waals component is determined using a linear relationship Eq. (4) between the van der Waals free energy of a given atom, i, ($\Delta G_{vW,i}$) and its exposed surface (S_i). In Eq. (4), the atomic surface tension (ξ_i) is obtained by fitting experimental free energies of solvation for small and medium-sized molecules that contain prototypical functional groups. Parametrized models for water [19], carbon tetrachloride [20], chloroform

[21], and n-octanol [22] are available.

$$\Delta G_{vW} = \sum_{i=1}^{N} \Delta G_{vW,i} = \sum_{i=1}^{N} \xi_i S_i \tag{4}$$

The electrostatic term is determined treating the solvent as a continuum polarizable medium, which reacts against the solute charge distribution generating a reaction field. This reaction field is introduced as a perturbation operator, V_R, into the Schrödinger equation Eq. (5). Such an operator is expressed in terms of a set of imaginary charges spread over the solute cavity Eq. (6), which are obtained by solving the Laplace equation with suitable boundary conditions Eq. (7). In Eq. (6) M is the total number of surface elements, j, in which the solute/solvent boundary is divided, and $\{q_j\}$ is the set of charges (located at r_j) that represent the solvent response. In Eq. (7), V_T is the total (solute + solvent) electrostatic potential, n is the unit vector normal to the surface of element j, and ε is the solvent dielectric constant.

$$(H^o + V_R)\Psi = E\Psi \tag{5}$$

$$V_R = \sum_{j=1}^{M} \frac{q_j}{|r_j - r|} \tag{6}$$

$$q_j = -\frac{\varepsilon - 1}{4\pi\varepsilon} S_j \left(\frac{\partial V_T}{\partial n} \right)_j \tag{7}$$

The electrostatic contribution to ΔG_{sol}, is then computed as noted in Eq. (8), where the index "sol" means that the perturbation operator is adapted to the fully relaxed charge distribution of the solute in solution, and the index "0" stands for the gas phase environment.

$$\Delta G_{ele} = \left\langle \Psi^{sol} \middle| H^o + \frac{1}{2} V^{sol} \middle| \Psi^{sol} \right\rangle - \langle \Psi^o | H^o | \Psi^o \rangle \tag{8}$$

By using a perturbational treatment of the electrostatic coupling between solute and solvent [23–25], Eq. (8) can be rewritten as noted in Eq. (9). According to Eq. (9), ΔG_{ele} is half the interaction energy between the gas phase charge distribution of the solute and the fully polarized solvent reaction field.

$$\Delta G_{ele} = \left\langle \Psi^o \middle| \frac{1}{2} V^{sol} \middle| \Psi^o \right\rangle \tag{9}$$

The translation of Eq. (9) to a classical framework is straightforward, since ΔG_{ele} is represented here only in terms of Coulomb integrals. This is shown in Eq. (10), where the charge distribution in the gas phase is represented by a set of point atomic charges $\{Q_i^o\}$ centered at r_i. Nevertheless, note that the charges that represent the solvent reaction field, q_j^{sol} Eq. (6), are determined from the fully polarized charge distribution of the solute, which is also represented by a set of atomic point charges $\{Q_i^{sol}\}$, *i.e.*, $q_j^{sol} = q_j^{sol}(\{Q_i^{sol}\})$. Equation 10 is denoted as the semiclassical approach. It retains all the main features of the solute–solvent electrostatic coupling, including mutual polarization effects, through the assignment of the solute charges $\{Q_i^o\}$ and $\{Q_i^{sol}\}$. These two sets of charges (typically atom-centered) are determined by simultaneously fitting the electrostatic potential and field (ESPF charges) computed at the solute/solvent interface [15].

$$\Delta G_{ele} = \frac{1}{2}\sum_{i=1}^{N}\sum_{j=1}^{M}\frac{Q_i^o q_j^{sol}}{|r_j - r_i|} \tag{10}$$

2.3. Configurational Search

Sampling of the configurational space is performed with the Metropolis Monte Carlo algorithm using the effective energy defined in Eq. (1). Because a continuum model is used to describe solvent effects, the unique explicit degrees of freedom are those defined for the solute, which allows for an exhaustive exploration of the solute configurational space compared to standard discrete MC or MD methods. To make the sampling more efficient, the MC-MST method uses a "multiple-copy" strategy [26], where several independent calculations are performed simultaneously, each starting from a different configuration of the solute. These configurations are randomly selected from a preliminary MC-MST calculation performed at high temperature. The multiple-copy strategy facilitates the sampling of the configurational space, as it is less dependent on the starting coordinates that a standard single ("single-copy") calculation.

3. MC-MST STUDY OF MOLECULAR ASSOCIATION

Previous applications of the MC-MST method have dealt with the dimerization of model compounds [26–28] that incorporates structural elements

typically exploited in host–guest complexes. The systems examined include formic acid, benzene, and the ionic pair between ammonium and formate, among other compounds.

A salt bridge is strongly dependent on the environment [26], since the Coulombic attraction between cation and anion is counterbalanced by the solvation of the separate ions. Thus, whereas near all the ion pairs have a separation less than 3 Å in the gas phase, a very few pairs with the two ions separated less than 3 Å are found in water. In fact, only 44% of the sampled configurations have a cation–anion separation comprised between 3 and 6 Å in water according to MC-MST calculations.

The MC-MST results also show that the formation of hydrogen-bonds is also hindered by solvation. The doubly hydrogen-bonded complex of formic acid [26, 29], which is the predominant configuration ($>99\%$) in the gas phase, is negligible in aqueous solution. Even the population of the single hydrogen-bonded complex is predicted to be less than 2% in water. In fact, the MC-MST results indicate that there is not a well-defined recognition pattern for the association of the formic acid in water. The relative orientation of the monomers is very variable, thus revealing the weakness and poor specificity of their interaction in aqueous solution.

Solvation also influences the interaction of two benzene molecules [26], but its effect is less relevant than for hydrogen-bonded complexes or ion pairs. Thus, neither the population of bonded pairs nor the nature and weight of the different interaction modes are largely altered upon hydration. These results demonstrate that the MC-MST method reflects qualitatively the effect of the polarity and hydrogen-bond donor/acceptor properties of water molecules on both the population of bonded pairs and the nature of the complexes.

From a quantitative point of view, the MC-MST method can also give an accurate description of the molecular association. Thus, in the dimerization of formamide in the gas phase [28] near 97% of the configurations correspond to "bound" dimers (around 62% and 35% of doubly and singly hydrogen-bonded complexes, respectively). Accordingly, the free energy of dimerization is predicted to be -2.5 kcal/mol (a correction of -0.4 kcal/mol for volume effects is also included). This estimate agrees with high level quantum mechanical values, which range from -2.0 to -3.2 kcal/mol. Hydration largely reduces the number of "bound" dimers. Thus, in water around 14% of the sampled configurations can be defined as bonded complexes, and only a fraction (around 1%) are hydrogen-bonded dimers. Accordingly, the predicted free energy of dimerization (0.7 kcal/mol) indicates that dimerization is not favored in water, in agreement with the

experimental evidence. Apparently, the experimental free energies of dimerization for diverse amides are even less favorable, since the values reported from IR measurements range between 2.5 and 3.5 kcal/mol [30, 31]. However, if we define a dimer considering only the population of hydrogen-bonded dimers, a definition that is likely closer to what is detected in IR experiments, the free energy of dimerization predicted from the MC-MST results amounts to 2.4 kcal/mol, in very good agreement with experimental evidence.

4. CONFORMATIONAL EQUILIBRIA

As noted above, the conformational equilibria of flexible molecules can be greatly affected upon solvation. To investigate the suitability of the MC-MST method to reflect the conformational change occurring upon solvation, we have studied two systems well characterized both experimentally and theoretically: 1,2-dichloroethane and the N1—H and N3—H tautomers of neutral histamine.

4.1. 1,2-Dichloroethane

The *gauche*/*trans* equilibrium of 1,2-dichloroethane (DCE) is altered upon solvation, the gauche conformer being favored as the solvent's polarity increases [32–36]. To investigate the influence of solvation on the *gauche*/*trans* equilibrium, MC-MST calculations of DCE in gas phase, chloroform, and aqueous solution were performed. The internal degrees of freedom were explored using two force–fields. First, the united-atom (UA) model of DCE parametrized by Jorgensen and coworkers [32] by fitting the gas-phase data on the barrier height and *gauche*/*trans* energy difference. Second, an all-atom (AA) model built up from standard parameters in the AMBER force–field [37], which were adjusted to reproduce the preceding gas phase data. The semiclassical MST model (Eqs. (3), (4) and (10)) was used to compute the free energy of solvation. ESPF charges obtained from the wavefunctions of the solute in the gas phase and in solution (determined using the MST HF/6-31G(d) method) were employed to compute the electrostatic component of ΔG_{sol}. Calculations were performed with the ESPF charges determined for the *trans* conformer, which were similar to those obtained for the gauche conformer. Cavitation and van der Waals components of ΔG_{sol} were determined using the standard parameters in the MST HF/6-31G(d) model.

MC-MST calculations were carried out using the multiple-copy strategy. To this end, twelve MC-MST simulations starting from structures randomly selected from a previous MC-MST calculation performed in the gas phase at high temperature (1000 K) were performed. Each simulation consisted of a total of 4 10^5 configurations. Similar results were obtained in every independent run, which allows direct averaging of the results obtained for the different trajectories (the shape of the minima was assumed to be similar).

The free energy profiles for the C1—C—C—C1 rotation determined from the population distribution in the gas phase, chloroform and water are shown in Figure 1. The plots show a symmetrical profile, which indicates that the conformational space has been sampled properly. The change in the

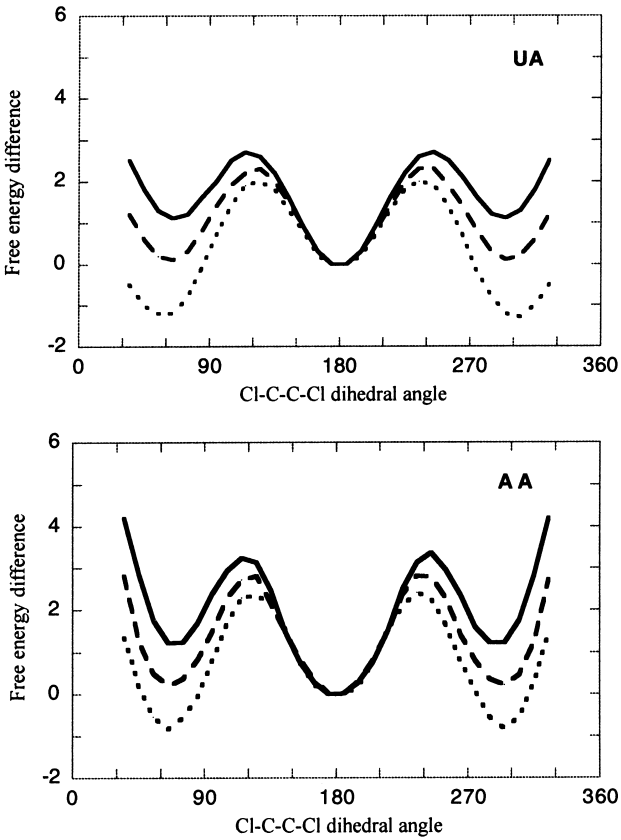

FIGURE 1 Free energy profiles (kcal/mol) for rotation about the C1—C—C—C1 dihedral angle (degrees) in 1,2-dichloroethane determined from the population distributions in the gas phase (solid line), in chloroform (dashed line), and in aqueous solution (dotted line).

population of the *gauche* and *trans* conformers induced upon solvation is clearly seen. Such a change is explained by the larger dipole moment of the *gauche* conformer compared to that of the *trans* form [32–37]. Note that the average dihedral angle for the *gauche* conformer decreases with increasing solvent polarity (from 65.1 and 72.8 degrees in the gas phase to 58.1 and 65.6 degrees in water according to the UA and AA results, respectively), in agreement with previous studies [34, 35]. This subtle conformational change enlarges the dipole moment of the *gauche* conformer (around 0.1 Debyes at the HF/6-31G(d) level), thus favoring its solvation in water (around 0.2 kcal/mol using the MST HF/6-31G(d) method).

Table I compares the MC-MST free energy difference between *gauche* and *trans* conformers with those obtained either experimentally or from other theoretical methods. The estimated free energy difference in chloroform (around −0.2 kcal/mol) and water (around −0.9 kcal/mol) agrees with the results predicted by other theoretical methods. The barrier for the *trans* → *gauche* conversion is lowered in condensed phases compared to the gas phase value (see Fig. 1), as expected from the better solvation of the *gauche* conformer compared to the *trans*. These trends also agree with the changes in the free energy profiles for the C1—C—C—C1 rotation determined from MC-free energy perturbation simulations [35]. The results show the large influence of solvation on the relative population between minima, but also on the general shape of the conformational free energy surface.

4.2. Histamine

The primordial biological activity of histamine has stimulated a number of studies about the relationship between its tautomeric and conformational properties and the pharmacological action [38–48]. Compared to 1,2-

TABLE I *Gauche*/*trans* free energy differences (kcal/mol) for 1,2-dichloroethane at 298 K determined experimentally and from theoretical computations

Medium	ε	*exptl.*[a]	*MC-FEP*[b]	*SCRF*[a,c]	*MC-MST*(*UA*)	*MC-MST*(*AA*)
Gas	1.0	1.20	1.2	1.2	1.1	1.2
Cyclohexane	2.0	0.70	1.1	0.8		
Di-n-butyl ether	3.1	0.51	0.7	0.6		
Chloroform	4.7				0.1	0.3
Tetrahydrofuran	7.6	0.11	−0.1			
Acetone	20.7	−0.14		0.1		
Acetonitrile	36.0	−0.22	−0.3	0.0		
Water	78.4				−1.0	−0.8

[a] Wiberg *et al*., *J. Phys. Chem*., 1995, **99**, 9072.
[b] Jorgensen *et al*., *J. Am. Chem. Soc*. 1995, **117**, 11809.
[c] B3LYP/6-311++G(d,p).

dichloroethane, the study of the conformational properties of histamine is more interesting owing to (i) the larger flexibility and (ii) the involvement of an internal hydrogen-bond.

The conformational preference of histamine has been examined from X-ray crystallography [41], NMR [42, 43] and IR [44] studies in solution, jet spectroscopy [45, 46], and molecular orbital calculations [47–48]. Here we focus our attention to the conformational properties of the N1—H and N3—H tautomers of neutral histamine, whose flexibility is determined by the three torsional parameters (τ_1, τ_2, τ_3) that define the conformation of the side chain (see Fig. 2). These dihedral angles are defined in such a way that the origin is in the *syn* arrangement (τ_1 is defined *syn* with regard to the proximal nitrogen atom). The internal energy was evaluated using the AMBER force field [37]. To this end, the force field was defined by mixing the corresponding parameters of the imidazole ring of the two tautomeric forms of neutral hystidine and those of the side chain of lysine. Charges on the methylene groups of histamine were adjusted as to maintain neutrality of the molecule. Seven MC-MST simulations, each consisting of 10^6 configurations, were run in the gas phase and in water using the same set-up procedure mentioned above for 1,2-dichloroetane. Similar results were obtained in every independent run, which supports convergence in the conformational search. A Boltzmann-weighted average of the different trajectories was performed to derive the global results.

Regarding the N1—H tautomer, the conformational flexibility of the side chain is well defined in the gas phase (see Fig. 3). The torsion τ_1 adopts values close to 30 or 330 degrees, and the minimum in its population

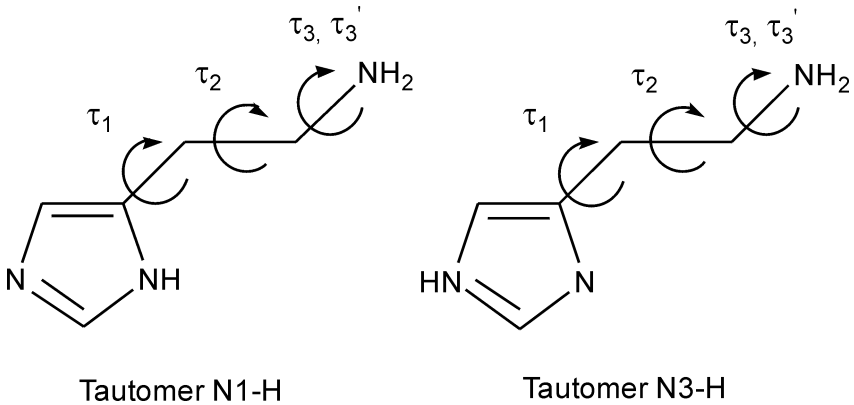

FIGURE 2 Torsional parameters defining the conformers of N1—H and N3—H tautomers of neutral histamine.

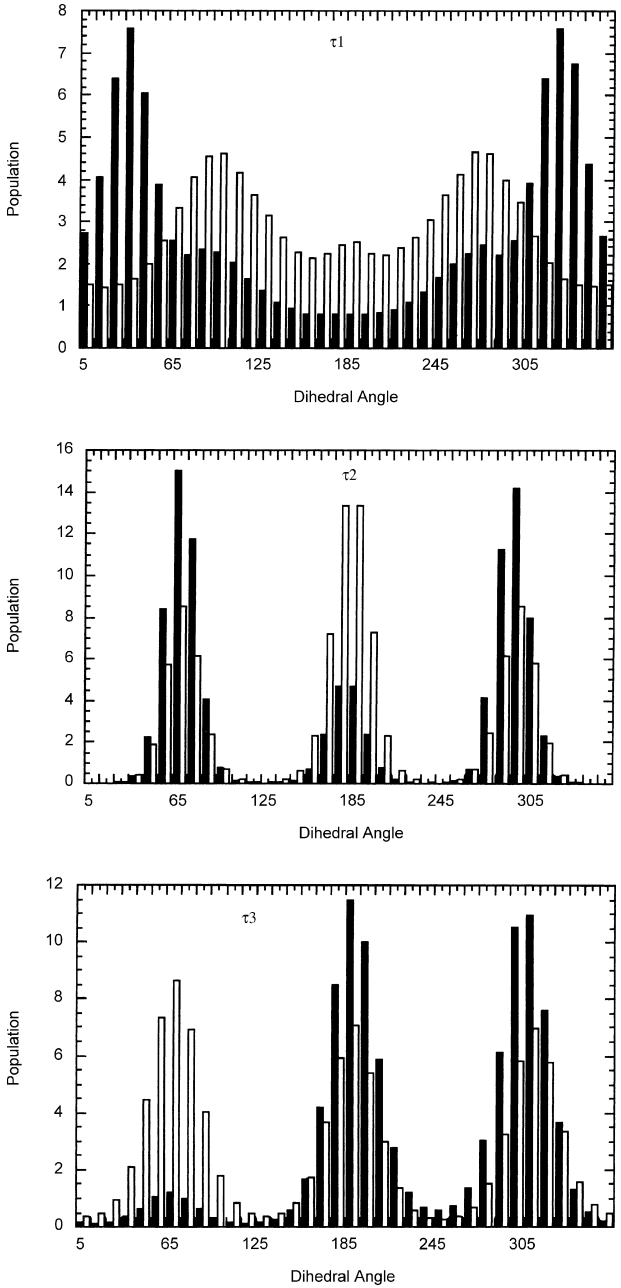

FIGURE 3 Population distribution (%) of the torsional parameters (degrees) for the N1—H tautomer of histamine in the gas phase (black) and in water (white).

distribution corresponds to the region around 180 degrees. The torsion τ_2 is mostly found in regions close to 60 or 300 degrees, and there is a small fraction in the region around 180 degrees. Likewise, the torsion τ_3 is located close to 180 or 300 degrees, while a very small fraction population is found around 60 degrees. These results imply the existence of a majoritary fraction of molecules having an intramolecular hydrogen-bond between the nitrogen atoms of the side chain amino and the ring NH groups. This is confirmed from inspection of Figure 4, which shows that the distance distribution between those nitrogen atoms has a maximum at around 2.9 Å. Therefore, the results indicate that the side chain of the N1—H tautomer adopts preferentially a *gauche* ($\tau_2 = 60$ or 300 degrees) conformation.

Table II shows the most populated conformational families of the N1—H tautomer in the gas phase. The largest fraction corresponds to internally hydrogen-bonded structures (around 45% of the sampled structures). Among the non-hydrogen bonded structures, *gauche* conformers with the side chain normal to the imidazole ring are the most populated. These results agree with both experimental data obtained from jet spectroscopy [45, 46] and quantum mechanical results [47, 48], which point out the hydrogen-bonded *gauche* conformer to be the most stable species of the N1—H tautomer in the gas phase.

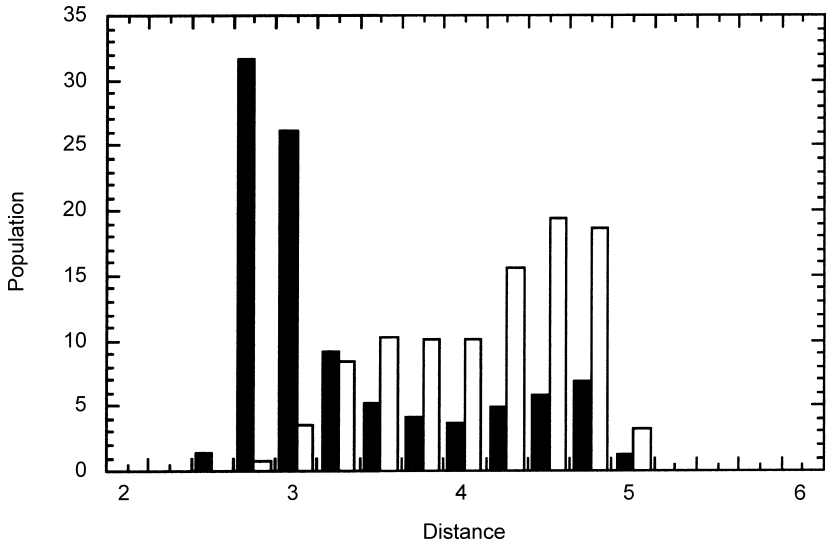

FIGURE 4 Population distribution (%) of the distance (Å) between the nitrogen atoms of the side chain amino and ring NH groups for the N1—H tautomer of histamine in the gas phase (black) and in water (white).

TABLE II Population of the most important conformational families of the N1—H tautomer of neutral histamine in the gas phase and in water[a]

	τ_1	τ_2	τ_3	D	α	%
Gas phase	330 (30)	60 (300)	150–210	3.0	120	28.6
	330 (30)	90 (270)	180–210 (150–180)	3.1	123	7.5
	300 (60)	90 (270)	180–210 (150–180)	3.1	120	6.9
	0	60 (300)	300–330 (30–60)	3.0	113	6.7
	300 (60)	60 (300)	180–210 (150–180)	3.0	116	6.3
	270 (90)	60 (300)	270–300 (60–90)	3.3	90	4.4
	240 (120)	60 (300)	300 (60)	3.7	72	2.1
	270 (90)	180	180	4.7	84	1.0
Water	270 (90)	180	60,180,300	4.7	83	5.6
	270 (90)	60 (300)	60,90 (270,300)	3.4	87	3.1
	240 (120)	60 (300)	60,90 (270,300)	3.7	72	3.0
	300 (60)	180	60,180,300	4.5	90	4.0
	240 (120)	180	60,300	4.9	76	3.1
	300 (60)	300 (60)	60,180	3.7	72	2.6
	270 (90)	300 (60)	180	4.0	61	1.3
	210 (150)	180	60 (300)	4.9	74	1.2
	330 (30)	300 (60)	180	3.5	86	1.0

[a] Torsional parameters τ_1, τ_2 and τ_3 (degrees; see Fig. 2), average distance between the nitrogen atoms in the amino and NH groups (Å) and N···HN angle (degrees), and the population of the conformer. For every internal torsion, the torsional space was partitioned in 12 windows (each window spans a range of 30 degrees) centered at 0, ±30, ±60, ±90, ±120, ±150, and 180, and every conformer was classified into one of those conformational families according to their torsional parameters. Only those conformational families populated more than 1% are indicated, though they are grouped when they differ exclusively in the torsion τ_3.

Solvation in water has a dramatic effect on the conformational preference of the N1—H tautomer (see Fig. 3). The torsion τ_1 mainly adopts values close to 90 or 270 degrees. Similarly, there is a large increase in the number of structures with $\tau_2 = 180$ degrees, which is accompanied by a notable reduction in the *gauche* population. Finally, the distribution of τ_3 is characterized by the presence of three similar maxima centered at 60, 180 and 300 degrees. There is a reduction in the number of hydrogen-bonded structures, as noted in the fact that the distance between the amino and NH nitrogens reaches a maximum in the population distribution located at around 4.6 Å (see Fig. 4). The loss of the internal hydrogen-bond upon hydration is accompanied by an increase in the conformational flexibility, as can observed in the torsional parameters of the conformational families collected in Table II. The population of *trans* conformers is clearly larger in water than in the gas phase, which can be understood from the favorable hydration of the polar groups. Though there is not quantitative data about the *trans*/*gauche* ratio of the neutral N1—H tautomer in water, the two species can expected to exist in solution according to the available experimental data [44].

The conformational properties of the N3—H tautomer can be examined from inspection of Figures 5 and 6. In the gas phase, the torsion τ_1 adopts

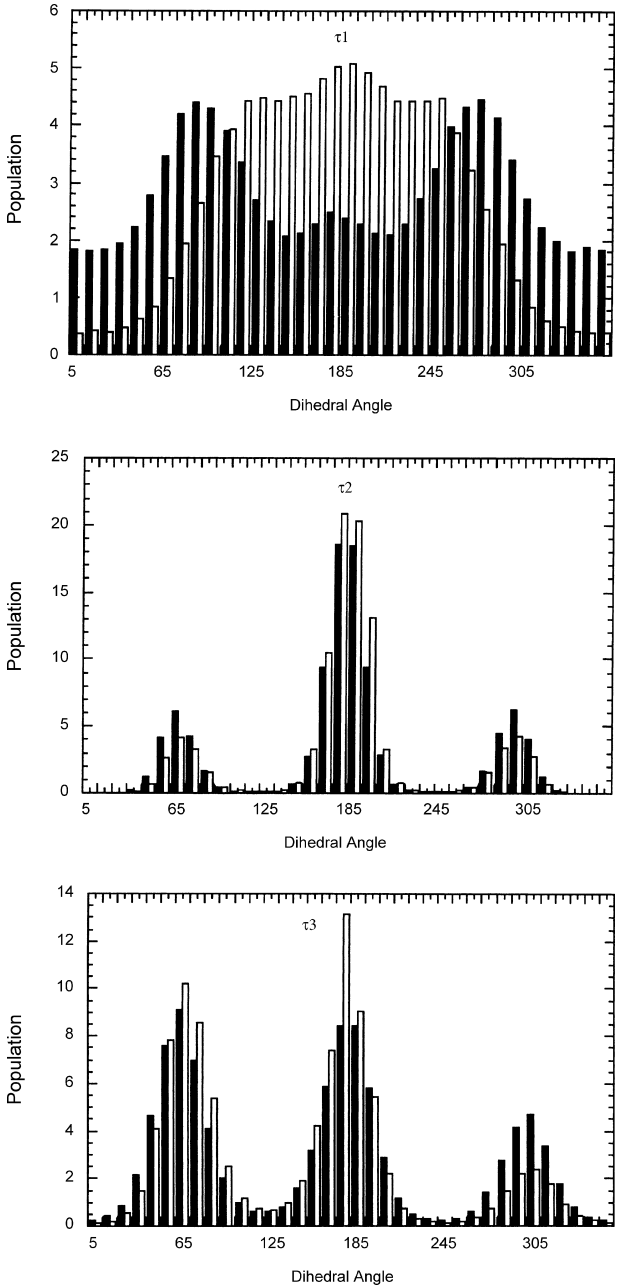

FIGURE 5 Population distribution (%) of the torsional parameters (degrees) for the N3—H tautomer of histamine in the gas phase (black) and in water (white).

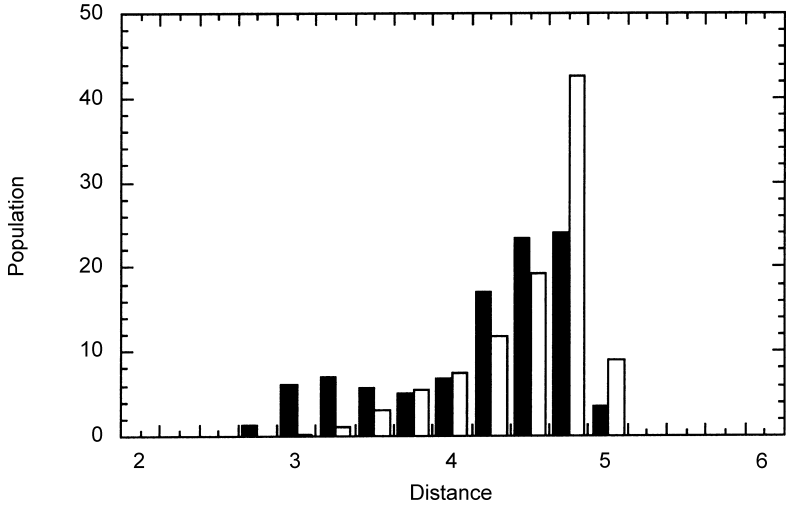

FIGURE 6 Population distribution (%) of the distance (Å) between the nitrogen atoms of the amino and N groups for the N3—H tautomer of histamine in the gas phase (black) and in water (white).

values close to 90 or 270 and at less extent 180 degrees. The torsion τ_2 is mainly in the region around 180 degrees, though there are significant population in the g*auche* (60, 300) region. Finally, the torsion τ_3 populates regions close to 60 and 180 degrees, and at less extent 300 degrees. Therefore, MC-MST results point out relevant differences in the conformational properties of N3—H and N1—H tautomers in the gas phase, in agreement with both experimental [45, 46] and theoretical [46–48] data. Thus, the predicted energy difference (calculated at the MP2/6-311++G(d, p)//MP2/6-31G(d, p) level) between the most stable *gauche* and *trans* forms decreases from around 5 to 1 kcal/mol upon tautomerism from the N1—H form to the N3—H species [46]. However, whereas the *gauche* conformers are more populated than the *trans* forms, the MC-MST results predict the reverse trend. This discrepancy, which likely stems from the difficulty to describe properly the interaction of the amino group with the π-electron system that occurs in the *gauche* conformers [45, 47], points out the sensitivity of the results to the force–field parameters.

Compared to the N1—H tautomer, hydration has little influence on the conformational preference of the N3—H tautomer (see Figs. 5 and 6). The most remarkable effect is the tendency of the torsion τ_1 to adopt values close to 180 degrees. There is also a slight enlargement of the *trans*/*gauche* ratio

upon hydration, which can be understood from the better hydration of the polar groups, as can be inferred from experimental data [44].

The results presented here suggest that the MC-MST method, in spite of the simplicity of its formalism, can be powerful to examine the configurational free energy surface of solutes in condensed phases. A potential limitation of the method, nevertheless, would be the lack of information about solvent molecules that play relevant structural or functional roles (see, for instance, Refs. [49] and [50]), which could limit the accuracy of the method to predict conformational free energy differences between relevant conformational families. However, the method can be easily modified to introduce discrete solvent molecules, *i.e.*, the first solvation shell, into the simulation and to explore both internal and intermolecular degrees of freedom simultaneously in the simulation with little increase in computer expense. On the other hand, the neglect of the solvent's degrees of freedom allow us to obtain an exhaustive sampling at a low computational cost compared to MD and MC simulations using an explicit description of the solvent molecules. Thus, every independent run led to the same nature and population of the most relevant conformational families of the two tautomers of neutral histamine in aqueous solution. In addition, the efficiency of the conformational sampling in solution is comparable to that in the gas phase, as can be stated from inspection of Figure 7, which shows the evolution in the number of conformational families sampled along the MC-MST simulation.

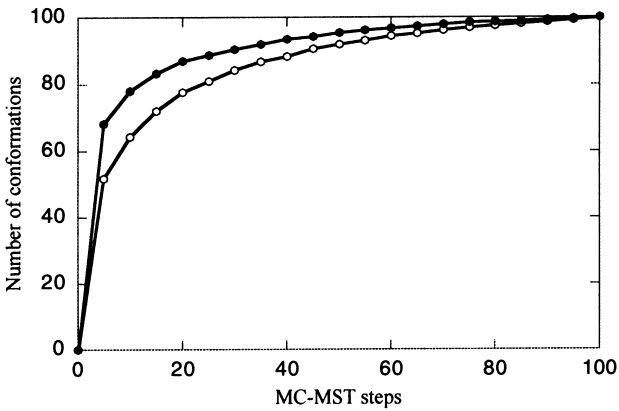

FIGURE 7 Number of conformational families (in percentage) sampled in the gas phase (white) and in water (black) as a function of the length of the MC-MST simulation (in units of 10^4 steps).

5. CONCLUDING REMARKS

The results presented in this article allow us to believe that the MC-MST method is able to provide, at least qualitatively, reliable representations of the conformational properties of flexible molecules in solution. Further support to our belief comes from previous studies based on continuum descriptions of the solvent [11–14], and particularly from the study reported by Varnek *et al.* [14], who implemented the Polarizable Contiuum Model in Molecular Dynamics simulations. Though there are differences between their continuum representation of the solvent and the semiclassical MST model presented here (*i.e.*, the treatment of non-electrostatic components of the free energy of solvation or the calculation of the mutual solute–solvent polarization), their results allow them to conclude that methods based on continuum models of the solvent can provide reliable descriptions of the conformational equilibria of molecules in condensed phases. Future investigations are needed to calibrate the reliability of the chemical description and the balance between accuracy and computational efficiency obtained from continuum-based approaches.

Acknowledgements

We thank the Dirección General de Investigación Científica y Técnica (projects PB98-1222 and PM99-0046) for financial support, and the Centre de Supercomputació de Catalunya (CESCA) for computational facilities. Fellowship from the Ministerio de Educación y Cultura to C. C. is kindly acknowledged.

References

[1] Cramer, C. J. and Truhlar, D. G. (1999). Implicit solvation models: equilibria, structure, spectra, and dynamics. *Chem. Rev.*, **99**, 2161–2200.
[2] Solvent effects and chemical reactivity. Tapia, O. and Bertrán, J. Eds.; Kluwer: Dordrecht, 1996.
[3] Structure and reactivity in aqueous solution. Cramer, C. J. and Truhlar, D. G. Eds.; ACS Symposium Series 568; American Chemical Society: Washington, 1994.
[4] Reichardt, C., Solvent and solvent effects in organic chemistry. VCH: Weinheim. 1998.
[5] Orozco, M. and Luque, F. J. (2000). Theoretical methods for the representation of solvent effects in biomolecular systems. *Chem. Rev.*, **100**, 4187–4225.
[6] Computer simulation of biomolecular systems. Theoretical and experimental applications. van Gunsteren, W. F., Weiner, P. K. and Wilkinson, A. J. Eds. Vol. 3. Kluwer: Dordrecth, 1997.
[7] Jorgensen, W. L. (1989). Free energy calculations: A breakthrough for modeling organic chemistry in solution. *Acc. Chem. Res.*, **22**, 184–189.

[8] Kollman, P. A. (1996). Advances and continuing challenges in achieving realistic and predictive simulations of the properties of organic and biological molecules. *Acc. Chem. Res.*, **29**, 461–469.
[9] Gao, J. (1996). Hybrid quantum and molecular mechanical simulations: An alternative avenue to solvent effects in organic chemistry. *Acc. Chem. Res.*, **29**, 298–305.
[10] Tomasi, J. and Persico, M. (1994). Molecular interactions in solution: An overview of methods based on continuous distributions of the solvent. *Chem. Rev.*, **94**, 2027–2094.
[11] Gilson, M. K., Davis, M. E., Luty, B. A. and McCammon, J. A. (1993). Computation of electrostatic forces on solvated molecules using the Poisson-Boltzmann equation. *J. Phys. Chem.*, **97**, 3591–3600.
[12] Wang, C. X., Wang, S. Z., Xiang, Z. X. and Shi, Y. Y. (1997). Incorporating hydration force determined by boundary element method into stochastic dynamics. *J. Phys. Chem. B*, **101**, 230–235.
[13] Friedrichs, M., Zhou, R., Edinger, S. R. and Friesner, R. A. (1999). Poisson-Boltzmann analytical gradients for molecular modeling calculations. *J. Phys. Chem. B.*, **103**, 3057–3061.
[14] Varnek, A. A., Wipff, G., Glebov, A. S. and Feil, D. (1995). An application of the Miertus-Scrocco-Tomasi solvation model in molecular mechanics and dynamics simulations. *J. Comput. Chem.*, **16**, 1–19.
[15] Luque, F. J. and Orozco, M. (1997). A new semiclassical continuum representation of solvation. *J. Phys. Chem. B*, **101**, 5573–5582.
[16] Miertus, S., Scrocco, E. and Tomasi, J. (1981). Electrostatic interaction of a solute with a continuum. A direct utilization of *ab initio* molecular potentials for the prevision of solvent effects. *Chem. Phys.*, **55**, 117–129.
[17] Pierotti, R. A. (1976). A scaled particle theory of aqueous and nonaqueous solutions. *Chem. Rev.*, **76**, 717–726.
[18] Claverie, P., Elaboration of approximate formulas for the interactions between large molecules. Applications in Organic Chemistry. In: *Intermolecular interactions*: *From diatomics to biopolymers*. Pullman, B. Ed. Wiley: New York, 1978. pp. 69–305.
[19] Orozco, M. and Luque, F. J. (1995). Development of optimized MST/SCRF methods for semiempirical calculations: The MNDO and PM3 hamiltonians. *J. Comput. Chem.*, **16**, 563–575.
[20] Luque, F. J., Bachs, M., Aleman, C. and Orozco, M. (1996). Extension of the MST/SCRF method to organic solvents: *Ab initio* and semiempirical parametrization for neutral solutes in CC14. *J. Comput. Chem.*, **17**, 806–820.
[21] Luque, F. J., Zhang, Y., Aleman, C., Bachs, M., Gao, J. and Orozco, M. (1996). Solvent effects in chloroform solution: Parametrization of the MST/SCRF continuum model. *J. Phys. Chem.*, **100**, 4269–4276.
[22] Curutchet, C., Orozco, M. and Luque, F. J. (2001). Solvation in octanol: Parametrization of the MST continuum model. *J. Comput. Chem.*, in press.
[23] Luque, F. J., Bofill, J. M. and Orozco, M. (1995). New strategies to incorporate the solvent polarization in self-consistent reaction field and free-energy perturbation simulations. *J. Chem. Phys.*, **103**, 10183–10191.
[24] Angyan, J. G. (1997). Comment on "New strategies to incorporate the solvent polarization in self-consistent reaction field and free-energy perturbation simulations". *J. Chem. Phys.*, **107**, 1291–1292.
[25] Orozco, M. and Luque, F. J. (1997). Generalized linear response approximation in discrete methods. *Chem. Phys. Letters*, **265**, 473–480.
[26] Colominas, C., Luque, F. J. and Orozco, M. (1999). Monte Carlo-MST: New strategy for representation of solvent configurational space in solution. *J. Comput. Chem.*, **7**, 665–678.
[27] Orozco, M., Cubero, E., Barril, X., Colominas, C. and Luque, F. J., Nucleic acid bases in solution. In: *Computational Molecular Biology*. *Theoretical Computational Chemistry*. Leszczynski, J., Ed. Vol. 8. Elsevier: New York, 1999. pp. 119–166.
[28] Colominas, C., Luque, F. J. and Orozco, M. (1999). Dimerization of formamide in gas phase and in solution. An *ab initio* MC-MST study. *J. Phys. Chem. A*, **103**, 6200–6208.
[29] Colominas, C., Teixido, J., Cemeli, J., Luque, F. J. and Orozco, M. (1998). Dimerization of carboxylic acids: reliability of theoretical calculations and the effect of solvent. *J. Phys. Chem. B*, **102**, 2269–2276.

[30] Klotz, I. M. and Franzen, J. S. (1962). Hydrogen bonds between model peptide groups in solution. *J. Am. Chem. Soc.*, **84**, 3461–3466.
[31] Krikorian, S. E. (1982). Determination of dimerization constants of *cis*- and *trans*-configured secondary amides using near-infrared spectrometry. *J. Phys. Chem.*, **86**, 1875–1881.
[32] Bigot, B., Costa-Cabral, B. J. and Rivail, J. L. (1985). Conformational equilibrium of 1,2-dichloroethane in methylchloride. A Monte Carlo simulation of the differential gauche-anti solvation. *J. Chem. Phys.*, **83**, 3083–3094.
[33] Jorgensen, W. L., Binning, R. C. Jr. and Bigot, B. (1981). Structures and properties of organic liquids: n-butane and 1,2-dichloroethane and their conformational equilibria. *J. Am. Chem. Soc.*, **103**, 4393–4399.
[34] Wiberg, K. B., Keith, T. A., Frisch, M. J. and Murcko, M. (1995). Solvent effects on 1,2-dihaloethane gauche/trans ratios. *J. A. Chem. Soc.*, **99**, 9072–9079.
[35] Jorgensen, W. L., McDonald, N. A., Selmi, M. and Rablen, P. R. (1995). Importance of polarization for dipolar solutes in low dielectric media: 1,2-dichloroethane and water in cyclohexane. *J. Am. Chem. Soc.*, **117**, 11809–11810.
[36] Vilaseca, E. (1996). Solvent effect on conformational equilibrium: A Monte Carlo study of 1,2-dichloroethane in carbon tetrachloride. *J. Chem. Phys.*, **104**, 4243–4257.
[37] Cornell, W. D., Cieplak, P., Bayly, C. I., Gould, I. R., Merz, K. M., Ferguson, D. M., Spellmeyer, D. C., Fox, T., Caldwell, J. W. and Kollman, P. A. (1995). A second generation force–field for the simulation of proteins, nucleic acids and organic molecules. *J. Am. Chem. Soc.*, **117**, 5179–5197.
[38] Ganellin, R. C. (1981). Medicinal chemistry and dynamic structure-activity analysis in the discovery of drugs acting at histamine H2 receptors. *J. Med. Chem.*, **24**, 913–920.
[39] Weinstein, H., Mazurek, A. P., Osman, R. and Topiol, S. (1986). Theoretical studies on the activation mechanism of the histamine H2-receptor: The proton transfer between histamine and a receptor model. *Mol. Pharmacol.*, **29**, 28–33.
[40] Luque, F. J., Illas, F. and Pouplana, R. (1987). On the mechanism of histamine H2 receptor activation. *Mol. Pharmacol.*, **32**, 557–563.
[41] Bonnet, J. J. and Ibers, J. A. (1973). The structure of histamine. *J. Am. Chem. Soc.* **95**, 4829–4833.
[42] Ganellin, C. R., Pepper, E. S., Port, G. N. J. and Richards, W. G. (1973). Conformation of histamine derivatives. 1. Application of molecular orbital calculations and nuclear magnetic resonance spectroscopy. *J. Med. Chem.*, **16**, 610–616.
[43] Ham, N. S., Casy, A. F. and Ison, R. R. (1973). Solution conformations of histamine and some related derivatives. *J. Med. Chem.*, **16**, 470–475.
[44] Byrn, S. R., Graber, C. W. and Midland, S. L. (1976). Comparison of the solid and solution conformations of methapyriline, tripelennamine, diphenhydramine, histamine, and choline. The infrared-X-ray method for determination of solution conformations. *J. Org. Chem.*, **41**, 2283–2288.
[45] Vogelsanger, B., Godfrey, P. D. and Brown, R. D. (1991). Rotational spectra of biomolecules: Histamine. *J. Am. Chem. Soc.*, **113**, 7864–7869.
[46] Godfrey, P. D. and Brown, R. D. (1998). Proportions of species observed in jet-spectroscopy–vibrational energy effects: Histamine tautomers and conformers. *J. Am. Chem. Soc.*, **120**, 10724–10732.
[47] Hernández-Laguna, A., Abboud, J. L. M., Notario, R., Homan, H. and Smeyers, Y. G. (1993). *J. Am. Chem. Soc.*, **115**, 1450–1454.
[48] Hernández-Laguna, A., Abboud, J. L. M., Homan, H., López-Mardomingo, C., Notario, R., Cruz-Rodríguez, Z., Haro-Ruiz, M. D. and Botella, V. (1995). *J. Phys. Chem.*, **99**, 9087–9094.
[49] Varnek, A. and Wipff, G. (1993). Dramatic solvent effect on the ligand wrapping around a complexed cation: A molecular dynamics study of p-tert-butylcalix[4]arene tetramide and its complexes with alkali cations and Eu3+ in acetonitrile. *J. Phys. Chem.*, **97**, 10840–10848.
[50] Troxler, L. and Wipff, G. (1994). Conformation and dynamics of 18-crown-6, cryptand 222, and their cation complexes in acetonitrile studied by molecular dynamics simulations. *J. Am. Chem. Soc.*, **116**, 1468.